ISSN PRINT 2319 1775 Online 2320 7876

Research paper UGC CARE Listed (Group -I) Journal Volume 10, Spl Iss 2, 2021

Numerical Modeling of Casson Fluid Flow with Magnetohydrodynamics (MHD) over an Inclined Porous Stretching Surface featuring Variable Properties.

M satish, Dept of mechanical, Koneru Lakshmaiah Education Foundation, India-522302,

Abstract

This study explores the dynamics of a Casson nanofluid flowing past an elongated sheet in the presence of chemical reactivity and thermal conductivity. The investigation employs partial differential equations (PDEs) to model the fluid flow, which are subsequently transformed into a system of ordinary differential equations. The numerical resolution of these modified equations is accomplished using the Runge-Kutta method in combination with shooting techniques. This can be attributed to the interplay between electrical conductivity (σ) and the magnitude of the magnetic force, resulting in an electromagnetic force that counteracts fluid motion. Consequently, an increase in the parameter Gm corresponds to a rise in mass buoyancy force, leading to a wider distribution of velocity. The study also highlights the effects of variable thermal conductivity and diffusion coefficient on temperature and concentration contours, respectively.

Introduction

Recent interest from prominent scholars has been drawn towards the significance of non-Newtonian fluid boundary layer flow in various industrial applications. These fluids are governed by intricate rheological equations, presenting substantial challenges for engineers and scientists seeking solutions. Among the array of non-Newtonian fluids, Casson fluid (visco-inelastic) has garnered particular attention due to its distinctive properties. Casson fluid is categorized as visco-inelastic, exhibiting a yield stress akin to blood, which underscores its non-Newtonian behavior. This distinct attribute plays a pivotal role in a range of applications, spanning from food and polymer processing to other industrial domains. Noteworthy contributions in this field include Mahanta and Shaw's three-dimensional analysis [1] of Casson fluid flow over a penetrable linearly stretching sheet, Kataria and Patel's investigation [2] into Casson fluid motion involving heat radiation and chemical reactions across an oscillating vertical lamina, and Ramana Reddy et al.'s study [3] on Casson and Maxwell fluids under the influence of non-uniform cross diffusion and heat source/sink. Furthermore, [4] recently delved into the dynamics of Casson fluid motion through a penetrable channel, while Idowu and Falodun [5] focused on the simultaneous flow of fluids with variable thermal conductivity and viscosity, exemplified by Casson and Walters-B fluids. In essence, these studies collectively underscore the intricate nature of non-Newtonian fluid dynamics, particularly within the context of Casson fluids, and shed light on their multifaceted applications in diverse industrial scenarios [6-8].

This study focuses on the outcomes arising from the influence of electromagnetic wave-induced radiation on the unsteady transport of heat and mass in a Casson fluid. The fluid exhibits persistent viscosity and encompasses factors such as viscous dissipation, magnetic field effects, and buoyancy forces. A comprehensive review of the existing literature reveals limited research attention devoted to this specific problem [9]. The combined effects of electromagnetic radiation and viscous dispersion hold significant implications in industrial engineering, ranging from applications in isotope separation and heat exchangers to petroleum reservoir management [10]. It is precisely these practical applications that underscore the importance and necessity of conducting this study.

ISSN PRINT 2319 1775 Online 2320 7876

Research paper UGC CARE Listed (Group -I) Journal Volume 10, Spl Iss 2, 2021

Mathematical formulation

Contemplate an inclined and elongated porous sheet, permeable in nature, which hosts an inherently unstable two-dimensional laminar boundary layer. Within this boundary layer, the motion is characterized by a viscous incompressible MHD Casson fluid. The sheet itself possesses elastic properties and contains perforations [11]. Additionally, the presence and distribution of chemical species are taken into account, revealing a scenario where heat is consistently imparted to the Casson nanofluid by these elements.

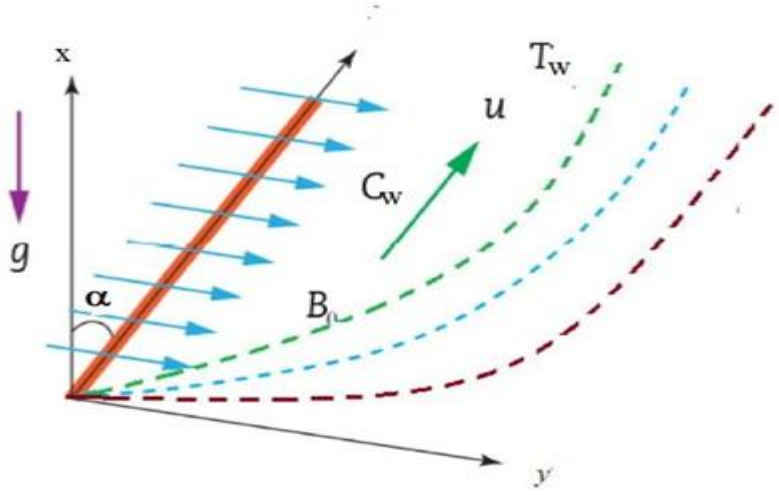

Figure 1: Physical geometry of the problem

The mathematical form for casson fluid is

$$\tau_{ij} = \begin{cases} 2\left(\mu_B + \frac{P_y}{\sqrt{2\pi}}\right) e_{ij}, \pi > \pi_c \\ 2\left(\mu_B + \frac{P_y}{\sqrt{2\pi_c}}\right) e_{ij}, \pi < \pi_c \end{cases} \quad (1)$$

ISSN PRINT 2319 1775 Online 2320 7876

Research paper UGC CARE Listed (Group -I) Journal Volume 10, Spl Iss 2, 2021

$$\frac{\partial u}{\partial x}+\frac{\partial v}{\partial y}=0\,, \tag{2}$$

$$\frac{\partial u}{\partial t}+u\frac{\partial u}{\partial x}+v\frac{\partial u}{\partial y}=\nu\left(1+\frac{1}{\beta}\right)\frac{\partial^2 u}{\partial y^2}-\left[\frac{\sigma B_0^2}{\rho}+\frac{\nu}{K}\right]u+\left[g\beta_T\left(T-T_\infty\right)+g\beta_C\left(C-C_\infty\right)\right]\cos\alpha\,, \tag{3}$$

$$\frac{\partial T}{\partial t}+u\frac{\partial T}{\partial x}+v\frac{\partial T}{\partial y}=\frac{\kappa}{\rho Cp}\frac{\partial^2 T}{\partial y^2}-\frac{\mu}{\rho Cp}\left(1+\frac{1}{\beta}\right)\left(\frac{\partial u}{\partial y}\right)^2-\frac{1}{\rho Cp}\frac{\partial q_r}{\partial y}\,, \tag{4}$$

$$\frac{\partial C}{\partial t}+u\frac{\partial C}{\partial x}+v\frac{\partial C}{\partial y}=D_M\frac{\partial^2 C}{\partial y^2}-Kc\left(C-C_\infty\right). \tag{5}$$

The boundary constraints are defined as in (6):

$$\text{At}\, y=0,\left\{u=u_w(x,t)=\frac{cx}{1-\lambda t},v=v_w(t),T=T_\infty+\frac{bx}{(1-\lambda t)^2},C=C_\infty+\frac{bx}{(1-\lambda t)^2}\right.$$

and as

$$y\to\infty u\to 0,T\to T_\infty,C\to C_\infty \tag{6}$$

where time is symbolized by t, whilst velocity components in the x-y plane are denoted by u and v and β is Casson fluid parameter.

The vitality condition (4) can be reduced by employing the Rosseland dispersion approach for the radiative flux as [12]:

$$q_r=-\frac{4\sigma^*}{3k^*}\frac{\partial T^4}{\partial y} \tag{7}$$

ISSN PRINT 2319 1775 Online 2320 7876

Research paper UGC CARE Listed (Group -I) Journal Volume 10, Spl Iss 2, 2021

$$T^4 = 4T_\infty^3 T - 3T_\infty^4 . \tag{8}$$

Heat flux can be estimated as

$$q_r = -\frac{16T_\infty^3 \sigma^* }{3k^* }\frac{\partial T}{\partial y} . \tag{9}$$

With the help of Eq (9), the energy equation (4) can appear as

$$\frac{\partial T}{\partial t} + u\frac{\partial T}{\partial x} + v\frac{\partial T}{\partial y} = \frac{\kappa}{\rho Cp}\frac{\partial^2 T}{\partial y^2} + \frac{\mu}{\rho Cp}\left(1+\frac{1}{\beta}\right)\left(\frac{\partial u}{\partial y}\right)^2 + \frac{1}{\rho Cp}\left(\frac{16T_\infty^3\sigma^*}{3k^*}\right)\frac{\partial^2 T}{\partial y^2} . \tag{10}$$

The below mentioned similarity transformation was initiated to reduce the mathematical analysis:

$$\eta = y\sqrt{\frac{c}{\nu(1-\lambda t)}}, \psi(x,y,t) = \sqrt{\frac{\nu c}{(1-\lambda t)}} x f(\eta), \frac{T-T_\infty}{T_w - T_\infty} = \theta(\eta), \frac{C-C_\infty}{C_w - C_\infty} = \phi(\eta), \tag{11}$$

by using the similarity transformation equation (11) for a nonlinear ordinary differential equations (ODE) system, the governing equations (3), (5), and (10) are transcribed in a non-dimensional form:

$$\left(1+\beta^{-1}\right) f''' - 0.5A\eta f'' + \left[A + K + M\right] f' + \left(f'\right)^2 - ff'' - Gr\theta - Gm\phi , \tag{12}$$

$$(1+R)\theta'' - \Pr\left[A(0.5\eta)\theta' + 2A\theta + f'\theta - f\theta' - Ec\left(1+\beta^{-1}\right)\left(f''\right)^2\right] = 0 , \tag{13}$$

$$\phi'' - Sc\left[A(0.5\eta)\phi' + (2A + Kr + f')\phi - f\phi'\right] = 0 . \tag{14}$$

The corresponding dimensionless form of boundary conditions are given by the equation:

$$\begin{aligned} &f = S,\ f' = 1,\ \theta = 1,\ \phi = 1 \quad \text{at} \quad \eta = 0 \\ &f' \to 0,\ \theta \to 0, \phi \to 0 \quad \text{as} \quad \eta \to \infty \end{aligned} \tag{15}$$

The skin-friction coefficient, Nusselt number (Nu), and Sherwood number (Sh) are the three basic physical characteristics that are taken into account:

$$Cf_x = \sqrt{\mathrm{Re}_x}\left(\frac{\mu}{\rho u_w^2}\left[\frac{\partial u}{\partial y}\right]_{y=0}\right), Nu = \left[\frac{x\kappa}{\sqrt{\mathrm{Re}_x}}\left(\frac{\partial T}{\partial y}\right)_{y=0}\right], Sh = \left[\frac{xD_M}{\sqrt{\mathrm{Re}_x}}\left(\frac{\partial C}{\partial y}\right)_{y=0}\right] . \tag{16}$$

Substituting Eq (11) into (16) to obtain the final dimensional form:

$$C_f = f''(0), Nu = -\theta'(0), Sh = -\phi'(0) \tag{17}$$

where $\mathrm{Re}_x = \frac{cx^2}{\nu(1-\lambda t)}$ stands for local Reynolds number, C_f is the local skin friction, Nu is the local

Numerical solution of the problem

For this, (12),(14) have been reduced to a system of seven initial problems of the first order of seven unknowns following the supposition in:

ISSN PRINT 2319 1775 Online 2320 7876

Research paper UGC CARE Listed (Group -I) Journal Volume 10, Spl Iss 2, 2021

$$f = f(1), f' = f(2), f'' = f(3), \theta = f(4), \theta' = f(5), \phi = f(6), \phi' = f. \quad (18)$$

Results

This investigation scrutinized the influence of heat and mass transfer on the dynamics of MHD Casson nanofluid with varying properties. The transformed equations (12)-(14), along with their corresponding boundary conditions as outlined in Equation (15), were mathematically solved employing a combination of Runge-Kutta methods and shooting techniques.

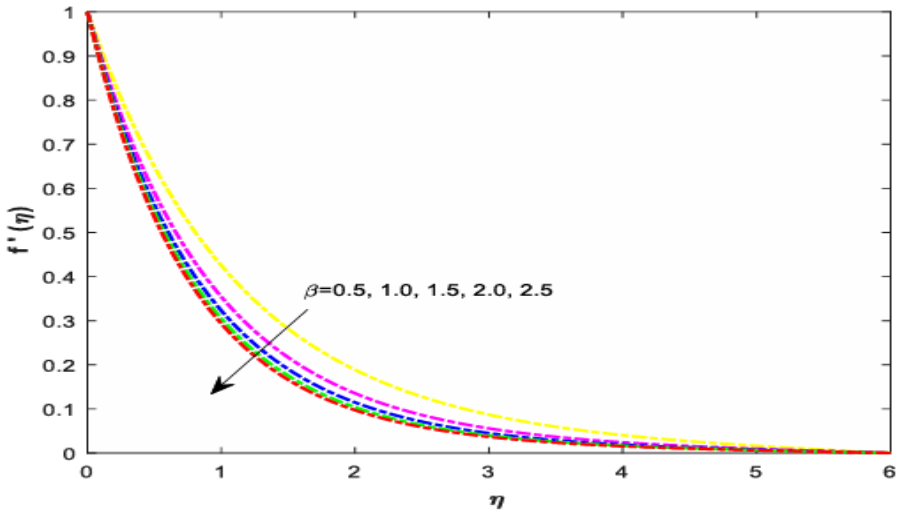

Figure 2: velocity profiles for different values of Casson parameter

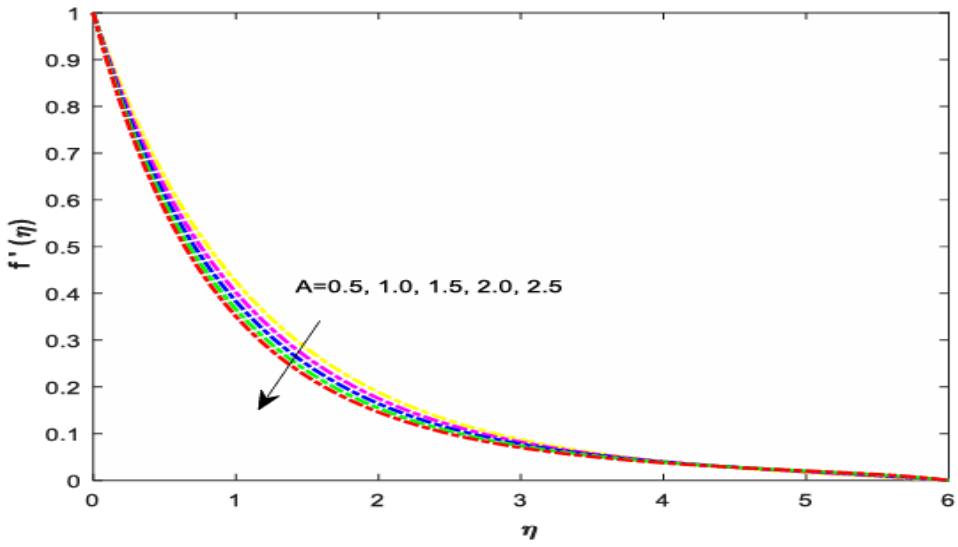

Figure 3: velocity profiles for different values of Unsteadiness parameter

Conclusion

ISSN PRINT 2319 1775 Online 2320 7876

Research paper UGC CARE Listed (Group -I) Journal Volume 10, Spl Iss 2, 2021

(i) Elevating the visco-inelastic parameter to a significant level result in the degradation of the velocity profile.

(ii) The development of the Lorentz force arises from the application of an attractive magnetic field. This force gains strength as the magnetic specification increases, giving rise to the emergence of an electromagnetic force.

(iii) Increasing the unsteadiness parameter (A) leads to the deterioration of velocity, temperature, and concentration distributions.

(iv) Amplifying the thermal radiation variable leads to an augmentation in the fluid's thermal state, subsequently enhancing the temperature contour.

References

1. G. Mahanta, S. Shaw, 3D Casson fluid flow past a porous linearly stretching sheet with convective boundary condition, Alex. Eng. J., 54 (2015), 653–659.
2. H. R. Kataria, H. R. Patel, Radiation and chemical reaction effects on MHD Casson fluid flow past an oscillating vertical plate embedded in porous medium, Alex. Eng. J., 55 (2016), 583–595.
3. J. V. Ramana Reddy, K. Anantha Kumar, V. Sugunamma, N. Sandeep, Effect of cross diffusion on MHD non-Newtonian fluids flow past a stretching sheet with non-uniform heat source/sink: A comparative study, Alex. and Eng. J., 57 (2018), 1829–1838.
4. A. S. Idowu, B. O. Falodun, Variable thermal conductivity, and viscosity effects on non-Newtonian fluids flow through a vertical porous plate under Soret-Dufour influence, Math. Comput. Simul., 177 (2020), 358–384.
5. L. Panigrahi, J. Panda, K. Swain, G. C. Dash, Heat and mass transfer of MHD Casson nanofluid flow through a porous medium past a stretching sheet with Newtonian heating and chemical reaction, Karbala Int. J. Mod. Sci., 6 (2020), 1–12.
6. K. Bhattacharyya, MHD stagnation-point flow of Casson fluid and heat transfer over a stretching sheet with thermal radiation, J. Thermodyn., 2013 (2013), 1–9.
7. T. Walelign, E. Gorfie, T. Kebede, A. Walelgn, Analytical study of heat and mass transfer in MHD flow of chemically reactive and thermally radiative Casson nanofluid over an inclined stretching cylinder, J. Phys. Commun., 4 (2020), 125003. https://doi.org/10.1088/2399-6528/abcdba
8. B. Falodun, F. D. Ayegbusi, Soret-Dufour mechanism on an electrically conducting nanofluid flow past a semi-infinite porous plate with buoyancy force and chemical reaction influence, Numer. Methods Partial Differ. Eq., 37 (2020), 1419–1438.
9. M. Kalteh, Investigating the effect of various nanoparticle and base liquid types on the nanofluids heat and fluid flow in a microchannel, Appl. Math. Model., 37 (2013), 8600–8609.
10. J. K. Kim, J. Y. Jung, Y. T. Kang, The effect of nano-particles on the bubble absorption performance in a binary nanofluid, Int. J. Refrig., 29 (2006), 22–29.
11. Saikumar, K. (2020). RajeshV. Coronary blockage of artery for Heart diagnosis with DT Artificial Intelligence Algorithm. Int J Res Pharma Sci, 11(1), 471-479.
12. Saikumar, K., Rajesh, V. (2020). A novel implementation heart diagnosis system based on random forest machine learning technique International Journal of Pharmaceutical Research 12, pp. 3904-3916.